Different water relations between flower and leaf periods: a case study in flower-before-leaf-emergence *Magnolia* species

Hui Liu[A,B], *Qiu-Yuan Xu*[A,C], *Marjorie R. Lundgren*[D], *Qing Ye*[A,B,E]

[A]Key Laboratory of Vegetation Restoration and Management of Degraded Ecosystems, South China Botanical Garden, Chinese Academy of Sciences, Xingke Road 723, Tianhe District, Guangzhou 510650, China.

[B]Guangdong Provincial Key Laboratory of Applied Botany, South China Botanical Garden, Chinese Academy of Sciences, Guangzhou 510650, China.

[C]University of Chinese Academy of Sciences, Yuquan Road 19A, Beijing 100049, China.

[D]Department of Animal and Plant Sciences, University of Sheffield, Sheffield S10 2TN, UK

[E]Corresponding author. Email: qye@scbg.ac.cn

Running head: Water relations in flower and leaf periods

Abstract: 284 (300 words)

Key words: 9

Content: ~6800 words

References: 64

Tables: 1

Figures: 5

Appendix: 1 table and 4 figures

Abstract. The differing water relations between flowers and leaves on a plant reflect the lack of coordination between reproductive and vegetative organs during the evolution of angiosperm species. Although the amount of water that flowers consume has been reported to vary across species, accurate measurements of flower water relations compared to that of leaves at the branch level are lacking, and how flowers regulate their hydraulic function and structure to maintain water balance remains unclear. To explore the ecophysiological basis underpinning the differences between flowers and leaves, we measured hydraulic and morphological traits and monitored sap flow in flowers and leaves from the same branches of two Magnoliaceae species that flower before leaf emergence (*Magnolia denudata* and *Magnolia soulangeana*). Sap flux density (J_S) of flowers was 22% and 55% of that predicted for leaves in *M. denudata* and *M. soulangeana*, respectively. J_S of flowers commenced before predawn and ceased early in the afternoon, reflecting their night-time flowering pattern and a dramatic decrease of J_S with increasing vapour pressure deficit (D) under the high light of midday. Relative to leaves, tepals were thicker and more hydrated, and had bigger but scarcer stomata, leading to lower stomatal conductance (g_s) and transpiration rate (E), less negative water potential (Ψ_{tepal}), and lower hydraulic conductance. This study revealed different hydraulic patterns in the flowers and leaves of the two *Magnolia* species. Although flowers consumed less than half the water that leaves did, they used different strategies to maintain sufficiently high Ψ to sustain hydraulic safety. *Magnolia* flowers retained more hydrated tepals by exhibiting less water loss than leaves via lower hydraulic conductance. In contrast, *Magnolia* leaves maintained high transpiration rates through efficient stomatal responses to environmental changes compared to flowers.

Additional keywords: floral hydraulics, flowering stage, gas exchange, leaf hydraulic conductance, Magnoliaceae, sap flow, stomata, water potential, xylem hydraulic conductivity.

Introduction

The primary function of flowers is reproduction and their development requires continuous supplies of water, nutrients and carbohydrates, transported via vascular systems from other organs (Galen *et al.* 1999; Chapotin *et al.* 2003; Feild *et al.* 2009b). Although flowers assimilate little carbon, they are located along the outer periphery of the tree canopy, an exposure that threatens desiccation. Thus to attract pollinators, flowers must maintain water balance and turgor to prevent wilting, although they may still transpire significant amounts of water and compete for resources with leaves (Roddy and Dawson 2012; Teixido and Valladares 2014). The coordination of activities between reproductive and vegetative organs within a plant is a fascinating topic (Gross and Soule 1981; Reekie and Bazzaz 1987; Lambrecht and Dawson 2007), yet virtually unknown from a hydraulic perspective. The water transport capacity of petals and leaves of angiosperm species evolved independently, as the vein length per area (VLA) of petals are consistent from basal to more derived lineages (Roddy *et al.* 2013), while VLA of leaves increased nearly threefold during angiosperm evolution (Brodribb and Feild 2010). Although pollinators impose important selection pressures on floral functional traits (Thien *et al.* 2009), the need to survive water limitation must surpass the need to attract pollinators (Feild *et al.* 2009a), and water relation traits are directly linked to floral maintenance. For example, a recent study of 11 orchid species reported that greater floral longevity required higher floral dry mass per area and more negative turgor loss points, but the morphological traits of flowers and leaves were independent (Zhang *et al.* 2017). They also found that flowers had more negative P50 (water potentials inducing 50% embolism of veins) than neighbouring leaves, a difference that was significant for two woody species but not two herbaceous ones (Zhang and Brodribb 2017). Therefore, the differing evolutionary trajectories of flowers and leaves suggest contrasting water relation strategies in the two organs, yet the differing amount of water consumption and underlying ecophysiology between flowers and leaves remain unclear.

The few studies that address water consumption in flowers indicate that this trait is highly variable across and within species (Whiley *et al.* 1988; Blanke and Lovatt 1993; Galen *et al.* 1999; Lambrecht *et al.* 2011; Lambrecht 2013; Roddy *et al.* 2016). For instance, Whiley *et al.* (1988) found that transpiration rate (*E*) of avocado (*Persea americana*) flowers was ~60% that of nearby leaves, while cuticular conductance was similar between flowers and leaves. However, another study found that *E* of avocado

flowers was higher than leaves, which was attributed to largely closed stomata and the waxy surfaces of avocado leaves, as well as the small, low density stomata on the flower petals (Blanke and Lovatt 1993). A delicate study using miniature sap flow sensors to separately quantify water use in single flowers and leaves found two understory species with nearly no sap flow to flowers, while water flow to flowers of two sun-exposed species was 30~50% that of nearby leaves (Roddy and Dawson 2012). However, all of these studies were based on species that simultaneous produce flowers and leaves by comparing *E* or sap flow at the tepal (*i.e.*, a collective name for flower parts that cannot easily be divided into sepals and petals) or leaf level, and accurate estimations of water use by flowers and leaves throughout entire trees has never been reported.

Determining separate flower and leaf traits across an entire tree is traditionally difficult. For example, estimates of total flower area are confounded when a large number of the flowers are unevenly distributed, and the tree has a dynamic flowering stage with different flowers continuously opening and fading quickly. One approach to separately estimate sap flow to each organ requires rremoving leaves during blossom time, but this method may redirect water to the remaining organs and increase both hydraulic conductance and *E* per area (Meinzer and Grantz 1990) and, as such, would not capture the actual flow partitioning between flowers and leaves in intact plants. By contrast, species with a natural flower-before-leaf-emergence (FBL) characteristic are ideal to study flower water consumption, as they can be directly measured and then later compared with water consumed by leaves on the same branch once leaves emerge.

There are over 70 FBL species commonly observed in China, most of which aggregated in large families such as the Magnoliaceae (esp. section *Yulania*), Rosaceae (esp. *Prunus*), and Fabaceae (esp. *Cercis*), while other FBL species are randomly distributed in different families (literature surveyed by the first author). FBL and early flowering are important strategies to occupy the cold early spring niche. Based on analyses of global datasets, selection favoured early flowering plants, and this selection pressure was stronger in temperate than tropical flora (Munguía-Rosas *et al.* 2012). In insect-pollinated species, early flowering and the thermogenesis of large flowers or inflorescences can attract more insects to achieve higher reproduction efficiency (Dieringer 1999; Seymour *et al.* 2003). Furthermore, due to their high

ornamental value, FBL species have been cultivated widely to produce larger, more fragrant and colourful flowers (Azuma *et al.* 1999).

The Magnoliaceae family is commonly used to study the evolution of flowering plants, with focuses on floral anatomy (Xu and Rudall 2006), pollination biology (Thien 1974; Azuma *et al.* 1999; Thien *et al.* 2000), and phylogenetics and geographical distributions (Qiu *et al.* 1999; Azuma *et al.* 2001; Kim and Suh 2013; Liu *et al.* 2016). Since Magnoliaceae species emerged prior to bee pollinators, their large flower size and floral thermogenesis co-evolved with beetle pollination (Thien 1974; Dieringer 1999; Gottsberger *et al.* 2012; Wang *et al.* 2014). FBL species in the Magnoliaceae only exist in sections *Yulania* and *Michelia* (subgenus *Yulania*) within the genus *Magnolia* (Figlar and Nooteboom 2004), and the flowering period of *Yulania* species are the earliest (February) among all the Magnoliaceae lineages (Law 2004). *Yulania* species also have very large flowers (*e.g.*, single tepal length and width are about 10 and 5 cm, respectively) compared with most flowering species and other FBL species (Dandy 1927; Law 2004). For these reasons, we chose to focus on section *Yulania* species in this study.

The two *Yulania* study species were grown in close proximity and flowered concomitantly in the South China Botanical Garden in Guangzhou, China. We monitored sap flow of branches in both species and microclimate conditions throughout flowering, leaf expansion and maturation periods, as well as daily gas exchange and water potential of tepals and leaves, and morphological and hydraulic traits associated with water transport. This research aimed to: (1) accurately quantify the water consumption by flowers and leaves of two *Yulania* species, taking advantage of the distinctive flower and leaf phenology of FBL species; and (2) investigate the water relations for flowers and leaves by integrating floral, leaf and stem hydraulic measurements. We hypothesized that (1) flowers would use less water per area than leaves of our study species, considering the lower temperatures during the flowering than vegetative period and previous findings that tepals have sparser stomata and lower E and hydraulic conductance than leaves in *Magnolia grandiflora* (Feild *et al.* 2009b); and (2) although flowers can regulate water loss by reducing stomatal conductance and tepal and stem water conductivities, these traits might be particularly sensitive to environmental change, causing flowers to avoid dehydration less efficiently than leaves.

Material and methods

Study site and species

Experiments were carried out in the South China Botanical Garden (SCBG) (23°11'N, 113°21'E, 20 m altitude) in Guangzhou, China, located in the low-subtropical monsoon climatic region where mean annual temperature is 21.2°C, spanning 13.6°C in January to 28.9°C in July. Mean annual precipitation is ~1700 mm, 80% of which occurs in the wet season between April and September.

The study species included *Magnolia denudata* Desr., a famous ornamental species with large white flowers and *Magnolia soulangeana* Soul.-Bod. 'Zhusha', a hybrid (*Magnolia denudata* Desr. × *Magnolia liliflora* Desr.) bred for ornamental purposes, which exhibits large showy purple flowers. Considering feasibility and the number of flower buds available, four *M. denudata* and eight *M. soulangeana* individual trees were selected for sap flow monitoring. Flowers of both species have 9 tepals arranged in 3 whorls, with many spirally arranged stamens in the center. All sampled individuals were mature trees, growing within 200 m^2 of the exhibition area in SCBG (Liu *et al.* 1997), ranging from 6 to 10 m in height, and 12 to 17 cm in diameter at breast height (DBH).

Flowering stage records, tepal and leaf area calculation

Flowering stage was recorded on six and ten branches from four and eight trees for *M. denudata* and *M. soulangeana*, respectively. Every day during the flowering period, we recorded the number of flowers on each branch in five custom classified stages: buds with bracts sealed, buds with bracts open, half-open flowers with bracts dropped, fully-open flowers, and faded flowers. We calculated the ratio of open flowers (*i.e.*, number of half and fully-open flowers/total number of flowers on a branch), and flower fading speed (*i.e.*, number of faded flowers/total number of flowers on a branch).

Allometric relationships between the basal stem diameter of a branch and the total flower or leaf area on that branch were evaluated using power functions. Because it is prohibited to prune large branches of these ornamental garden trees, we could only measure hydraulic traits on small branches (diameter ~10 mm) and then build models to predict flower and leaf areas on the large branches that we monitored. Total flower area on each branch was calculated as the total number of flowers × mean area of a single flower, which was the average value based on 15 fully-open flowers from

nearby branches for each species. Leaf areas on small branches (diameter <10 mm) were measured by a leaf area meter (Li-3000A; Li-Cor, Lincoln, NE, USA), and stem diameters were measured with a calliper. We also selected 15 large branches (diameter 10~40 mm) for each species, and measured the number and diameter of all small branches on them, such that total areas of leaves could be calculated from stem diameters for branches used for sap flow monitoring. We also recorded the average individual tepal and leaf areas, and thickness of leaves and tepals (*i.e.*, at the thickest and thinnest parts, since the base of a tepal is very thick and tapers to the upper margin).

Sap flow and environment monitoring

Sap flow was monitored on the same branches that we used to record flowering stage, using the heat balance method (Sakuratani 1981) with the Dynagage Flow32-1K system (Dynamax, Houston, TX, USA). Constrained by branches of a suitable diameter, length, and available straight segment without small branches, gauges were installed at different heights and directions along the trees within a 50 m diameter circle from each data logger. Every gauge and cable connection were waterproofed to avoid rainfall damage. The thermal conductance constant (K_{sh}) for each gauge was calibrated with the heat balance function between 01:00 and 05:00 on 2 to 3 days with heavy cloud or rain, when no sap flow was assumed to occur before the sunrise. Gauge outputs were measured every 60 s and recorded as 10-min means with a CR1000 data logger. The original data were sap flow (g hr^{-1}), which were transformed into sap flux density (J_S, g m^{-2} s^{-1}) by dividing sapwood area for each of the 16 branches. We modelled the relationships between sapwood area and stem diameter for the two species, based on data of smaller branches (diameter<15 mm) during the measurement of hydraulic conductivity, and data of larger branches (diameter 15~60 mm) from cores collected by a tree growth cone after removing the equipment to get accurate estimations for each branch. Monitoring occurred between Feb-19 and Mar-27, 2015, which encompassed the entire flowering (Feb-15 to Mar-10) and leaf growth (Mar-2 to Mar-20) periods. However, branches with fewer than five flowers showed sap flow values near zero during most of the flowering period, with the exception of some irregular high points. Only six larger branches showed regular daily dynamics (three *M. denudata* and three *M. soulangeana*), and were used in further analysis of sap flow during the flowering period.

An automatic weather station (ECH2O Utility, Decagon Devices Inc. WA, USA) was setup on the third floor roof about 100 m away from the experimental site, monitoring the environment every 60 s, and recording it as 10-min means. Meteorological data included air temperature (T, °C), relative humidity (RH, %), solar radiation (SR, W m^{-2}), and rainfall (mm) during the experimental period, with vapour pressure deficit (*D*, kPa) calculated as $a \times \exp[b \times T/(T+c)] \times (1-RH)$, where *a*, *b*, and *c* are fixed parameters as 0.611 kPa, 17.502 (unitless) and 240.97 °C, respectively.

Gas exchange and water potential

Gas exchange was measured on tepals and leaves over two sunny days; one in the middle of the flowering period (Feb-24, 11:00 and 16:00), and the other after most leaves had expanded (Mar-26, 7:00, 10:30, 13:00, 16:30 and 18:00). On five trees per species, we cut off one half-open and one fully-open flower from each tree using a tree pruner, avoiding flowers on the branches where we monitored sap flow. Flower stalks were immediately transferred into water and gas exchange rates were measured on tepals from three whorls (1^{st}, outer whorl; 2^{nd}, middle whorl; 3^{rd}, inner whorl). The sun-exposed branches were bent downward to access leaves for measurements. Five trees for each species were chosen, and four leaves on each tree were measured. The two species we studied have clusters of four leaves each in one of four growth stages (1^{st}, half-expanded leaves; 2^{nd}, fully-expanded leaves; 3^{rd}, mature leaves; 4^{th}, older basal leaves), thus we measured one representative leaf from each stage on each tree.

Stomatal conductance (g_s, mol m^{-2} s^{-1}) and transpiration rate (*E*, mmol m^{-2} s^{-1}) of tepals and leaves were measured with an open leaf gas exchange system (LI-6400, LI-COR, Lincoln, NE, USA). For daily dynamics, a chamber with a transparent lid was used to measure natural light conditions, while CO_2 concentration, T, RH, and *D* uncontrolled in the chamber, in order to calculate hydraulic conductance based on the real-time *E*. During gas exchange measurements, water potentials (Ψ, MPa) of tepals taken from the same flower, and of leaves taken from the same twig were measured using a pressure chamber (PMS, Corvallis, OR, USA). Stem water potential (Ψ_{stem}, MPa) was also measured, using leaves that were wrapped with foil and sealed in plastic bags the evening before measurement day.

Stem hydraulic conductivity

Early in the morning, terminal branches (8~10 mm in diameter) from five trees per species were excised. All stems were immediately recut under water and leaves were misted with water, before samples were sealed in black plastic bags with moist towels to prevent transpiration and quickly transported to the laboratory. A stem segment 20~30 cm in length was cut under water from each branch, and both cut ends were trimmed with a razor blade. Branch segments were first flushed with filtered and degassed 20 mmol KCl solution at a pressure of 0.1 MPa for 10 min to remove air embolism. Then hydrostatic pressure generated by a 50 cm hydraulic head drove water flow through the segments. The downstream end of each segment was connected to a pipette and the time for fluid in the pipette to cross a certain graduation was recorded. Hydraulic conductivity (K_h, kg m s^{-1} MPa^{-1}) was calculated as water flux through the segment divided by the pressure gradient driving the flow. Sapwood specific hydraulic conductivity (K_S, kg m^{-1} s^{-1} MPa^{-1}) was calculated as K_h divided by the sapwood cross section area (A_S). Leaf specific hydraulic conductivity (K_L, kg m^{-1} s^{-1} MPa^{-1}) is the ratio of K_h to the total leaf area attached to the stem segment (A_L). A_L was measured by a leaf area meter to calculate the leaf to sapwood area ratio (A_L/A_S, m^2 cm^{-2}). Sapwood samples with bark removed were saturated in water overnight, then after wiping the surface dry, the sapwood fresh volume was measured by the water displacement method. These samples were then oven-dried at 70 °C for 72 h and weighed to obtain dry mass. Sapwood density (WD, g cm^{-3}) was calculated as the ratio of dry mass to fresh volume from the same branches used for K_h measurements.

Tepal and leaf turgor loss point (Ψ_{tlp})

Pressure volume (PV) curve analysis, based on the bench drying method, was used to calculate turgor loss point (Ψ_{tlp}) for both tepals and leaves (Tyree and Hammel 1972). Terminal branches that contained tepals or leaves were excised from three to five trees per species, recut underwater, and rehydrated until water potential was greater than -0.05 MPa. Tepal and leaf weight, and Ψ were measured periodically during desiccation. After pressure-weight measurements, samples were oven-dried at 70 °C for 72 h, dry weight was used to calculate leaf (or tepal) dry matter content (LDMC, %), and Ψ_{tlp} was determined according to PV models with leaf relative water content (RWC) and $-\Psi^{-1}$ (Schulte and Hinckley 1985). The hydraulic safety margin (HSM, MPa) was calculated as the difference between minimum water potential (*i.e.*,

Ψ_{pm}) and Ψ_{tlp}. Relative capacitance at full turgor (C_{ft0}, MPa^{-1}) was calculated as Δ RWC/ $\Delta \Psi$ between full turgor and turgor loss point. Leaf (or tepal) area specific capacitance at full turgor (C_{ft}, mol m^{-2} MPa^{-1}) was standardized as $C_{ft0} \times$(leaf turgor mass－leaf dry mass)/leaf area (Sack *et al.* 2003).

Tepal and leaf hydraulic conductance (K_{tepal}; K_{leaf})

Although there are different methods to measure hydraulic conductance of detached tepals and leaves (Sack *et al.* 2002), our preliminary experimentation showed that the high-pressure method was not suitable for K_{tepal} measurement, since large amounts of mucilage in tepals may contribute to capacitance but may not increase conductance, which would result in unusually high K_{tepal} values. Thus we estimated K_{tepal} and K_{leaf} (mmol m^{-2} s^{-1} MPa^{-1}) based on the real-time transpiration and water potential data (*i.e.*, K_{tepal} and $K_{leaf} = E/(\Psi_{stem}-\Psi)$), which we used to represent the hydraulic conductance of tepals and leaves under natural conditions (Brodribb and Holbrook 2003).

Specific leaf (or tepal) area (SLA), nutrients and stomatal traits

Specific leaf area (SLA, cm^2 g^{-1}) was calculated as leaf area divided by leaf dry mass. For each species, 20 tepals and leaves were scanned using a leaf area meter then oven-dried at 70 °C for 72 h. Dried samples were ground and homogenized for nutrient measurements. Total nitrogen content (N, %) was determined by Kjeldahl analysis after digestion with concentrated H_2SO_4. Total phosphorus content (P, %) was analyzed by atomic absorption spectrum photometry (UV-6000; Metash, Shanghai, China).

Epidermal peels of fresh tepals and leaves were extracted using a sharp razor blade, then observed under a microscope equipped with a digital camera (Optec Instrument, Chongqing, China) and a computerized image analysis system (OPTPro2012 version 4.0, Optec software). Three epidermal peels from each of three flower whorls and four leaf growth stages were analyzed per species and, on each peel, three images were randomly chosen as replicates. Guard cell length (GL) and width (GW) were measured, and stomatal density (SD) was counted. The stomatal pore area index (SPI, %) indicated stomata pore area per leaf area, which equaled $SD \times GL^2$ (Sack *et al.* 2003). The maximum diffusive conductance to water vapour (g_{max}) was estimated as

transpiration potential, calculated as $(d/v)\times SD\times a_{max}/\ [(l+\pi/2\times\sqrt{(a_{max}/\pi)}]$ (Brown and Escombe 1900; Franks and Beerling 2009); where d is the diffusivity of water vapour in air at 25 °C ($m^2\ s^{-1}$); v is the molar volume of air at 25 °C ($m^3\ mol^{-1}$); SD is stomatal density; a_{max} is the maximum area of the open stomatal pore, estimated as $\pi\cdot(p/2)^2$ where p is stomata pore length and was approximated as GL/2 as in Franks and Beerling (2009); l is stomata depth for fully open stomata, approximated as GW/2; and π is the geometric constant. In *Magnolia* species, stomata exist on both the adaxial and abaxial surfaces of tepals, but only on the abaxial surface of leaves. Thus we combined the calculated SPI and g_{max} of both tepal surfaces to obtain total SPI and g_{max} values.

Data analyses

All data were analysed in R v3.0.3 (R Development Core Team 2013). First, we tested whether the tepal or leaf traits differed among the three flower whorl types or among the four leaf growth stages using one-way ANOVAs, such that values that differed significantly among flower whorls or leaf stages were then analysed using multiple comparisons (Tukey HSD) in the daily dynamic dataset. Next, the differences between flowers and leaves were tested using *t*-tests for each species separately. In the above tests, data were natural log-transformed to fulfil the requirement of normal distribution, using absolute value for traits with negative values (e.g. Ψ_{tlp}).

To quantify the relationships between J_S and D, we performed boundary line analyses (Chambers *et al.* 1985; Ewers *et al.* 2005). We used J_S data from days when flower opening ratios were stable and all leaves were expanded, filtering out data collected under limiting light (SR=0 W m^{-2}) and during low D (<0.1 kPa) when empirical relationships between canopy stomatal conductance (G_s) and D were not well constrained (Oren *et al.* 1999). This will enable the resulting boundary line to give the best estimate of hydraulic limitation to water flux because the boundary line occurred during conditions that lead to the highest G_s at any given D. Next, the relationships between J_S and D were examined using the boundary line analysis independently for data grouped by four (0~200, 200~400, 400~600, 600~800 W m^{-2}) and two (0~400, 400~800 W m^{-2}) light gradients, in order to examine light effects. We found that both flowers and leaves showed significantly different relationships between the two light gradients and, as such, we used low light (LL, 0~400 W m^{-2}) and high light (HL, 400~800 W m^{-2}) in the final analyses. We used log-linear models

to predict J_S from ln$D$, which could indicate the sensitivity of sap flow response to changes in D. Furthermore, considering similar SR conditions, and the range of D on Mar-26 (when in leaf) encompassed that measured on Feb-24 (when in flower), we predicted J_S of leaves based on the relationships between J_S of leaves and D for *M. denudata* and *M. soulangeana*, in order to directly compare J_S of flowers and leaves.

To quantify the sensitivity of g_s to D from the daily dynamic data, we selected morning (10:30-11:00) and afternoon (13:00-16:30) periods to compare flowers and leaves. According to Lohammar's function g_s=-k×ln$D$+b, where k is the sensitivity index and, b is a constant (Lohammar *et al.* 1980), we built models for each species in each time period. The relationships between g_s and Ψ for the daily dynamic data were also tested, but clear patterns were not found.

Results

Environments and sap flux density during flowering and vegetative periods

Flowering period had lower daily average D and T, but similar SR compared to the vegetative period (Fig. 1a, b). While there were several rainfall events that distinctively affected D and T, sunny days in both flowering and vegetative periods enabled the daily dynamic measurements of gas exchange and water potential. During the main flowering period, the average sapwood area based J_S was about 234 and 750 kg m^{-2} $day^{-1}$for *M. denudata* and *M. soulangeana*, respectively. In both species, J_S was clearly lower in the flowering period than the vegetative one (Fig. 1c, d),

The sunny day with only flowers (Feb-24) or leaves (Mar-26) on the tree elicited very different responses (Fig. 2). Daily D peaked at 13:00 during the flowering period and 16:00 in the vegetative period (Fig. 2a), due to T and RH patterns. Specifically, T was consistently 6.34±0.11 °C lower in the flowering than vegetative day, and RH decreased from 90% at 6:00 to a minimum of 60% at 13:00 in the flowering day, while RH in the vegetative day deceased from 95% at 6:00 to a minimum of 52% at 16:00. SR was similar in the mornings of flowering and vegetative periods, but was slightly lower after 13:00 in the flowering period (Fig. 2b). J_S was lower during the flowering period than the vegetative one, a pattern that was more dramatic in *M. denudata* than *M. soulangeana* (*i.e.*, daily accumulated floral water consumption was 17% and 53% that of leaves for *M. denudata* and *M. soulangeana*, respectively). J_S peaked around 10:00 during flowering period and around 14:00 during the vegetative period (Fig. 2c, d). Furthermore, although D was higher in vegetative than flowering

period (Fig. 2a), J_S of flowers was still smaller than that predicted for leaves in the flowering period, and daily accumulated floral water consumption was 22% and 55% that of leaves for *M. denudata* and *M. soulangeana*, respectively (Fig. S1).

Flowering stages

We selected periods with stable ratios of opening and fading floral stages for sap flow data analyses to avoid the variance brought by changing flower number. *M. denudata* flowered quickly and maintained a high open flower ratio (i.e., around 70%) for six days, after which the flowers all dramatically faded within four days (Fig. 3a, c). Meanwhile, the flowering stage of *M. soulangeana* was slow, maintaining only 30% open flowers for about a week. Although *M. soulangeana* then remained with a 40% open flower ratio after the initial seven days, the fading stage had already commenced and the majority of flowers (70%) quickly faded within three days (Fig. 3b, d).

Effects of vapour pressure deficit on sap flux density and stomatal conductance

J_S of flowers was more vulnerable to high light than J_S of leaves (Fig. 4). Under low light (LL), J_S of flowers initially increased, followed by a slight decrease with ln$D$, while under high light (HL), J_S of flowers decreased with ln$D$ for both species (Fig. 4a, b). On the other hand, J_S of leaves increased with rising ln$D$ at both light levels, with higher J_S under HL than LL (Fig. 4c, d). J_S of *M. denudata* leaves was much higher than that of its flowers, while the maximum J_S of *M. soulangeana* flowers was even higher than that of *M. soulangeana* leaves (Fig. 4).

In general, g_s of leaves was significantly higher than that of flowers, and leaf g_s was also more sensitive to changes in D (Fig. 5). In the morning, g_s in both flowers and leaves reached higher maximum values and decreased more dramatically with increasing ln$D$ than in the afternoon. In both morning and afternoon measurements, *M. soulangeana* showed higher sensitivity in tepal g_s to ln$D$, but lower sensitivity of leaf g_s to ln$D$, compared to *M. denudata* (Fig. 5).

Comparisons of plant traits between flowers and leaves

Flowers and leaves differed significantly in nearly all of the measured traits, with the exception of K_S and N and P contents (Table 1). Both single leaf area and total leaf area were greater than those of flower tepals, on branches at the same diameter scale (A_L/A_S in Table 1; Fig. S2). Leaves were thinner than even the thinnest parts of tepals,

with higher SLA and LDMC. Thus the averaged total water content amount for tepals and leaves standardized by sapwood area showed that: flowers stored more water than leaves on the same diameter branch (101.6 g cm^{-2} and 88.3 g cm^{-2} for *M. denudata* with flowers and leaves, respectively; 103.1 g cm^{-2} and 90.2 g cm^{-2} for *M. soulangeana* with flowers and leaves, respectively). Tepals had much larger but also rarer, stomata than leaves, which resulted in SPI and g_{max} of tepals to be only 3% and 2% that in leaves, respectively. However, the measured g_s and E of tepals were about 27% and 22% that of leaves for *M. denudata*, respectively, and up to 65% and 55% that of leaves for *M. soulangeana*, respectively. Compared to tepals, leaves had more negative Ψ_{am}, Ψ_{pm} and Ψ_{tlp}, and higher HSM in *M. denudata* but lower HSM in *M. soulangeana* (all the HSM>0). Leaves also had much lower C_{ft}, much higher K_{leaf} and smaller K_L than tepals (Table 1).

In addition, several traits differed by flower whorls or leaf growth stages in both study species, including leaf area, thickness, flower LDMC, g_s, E, flower Ψ, HSM and K_{leaf} (K_{tepal}). In contrast, single tepal area, Ψ_{tlp} and C_{ft} differed among flower whorls only in *M. soulangeana*. The remaining traits did not differ among whorls or stages (Table 1; Table S1). Specifically, single leaf area was smallest in the half-expanded or older basal leaves and largest in mature leaves. Tepal thickness of the 1st whorl was the thinnest and gradually increased from the 2nd to the 3rd whorl, while half-expanded leaves were thinner than other mature leaves. For LDMC of tepals, the 1st whorl had the highest values, followed by the 2nd and 3rd whorls, while the HSM of tepals was smallest in the 1st whorl. K_{tepal} increased between the 1st, 2nd and 3rd whorls, while K_{leaf} was lowest in the half-expanded leaves and highest in the full-expanded leaves, with mature and older leaves showing intermediate values (Table S1). For *M. soulangeana*, single tepal area was largest in the 2nd whorl, followed by the 3rd and 1st whorls, and both Ψ_{tlp} and C_{ft} increased from the 1st and 2nd whorls to the largest 3rd whorl. E among flower whorls and leaf stages showed the same pattern as g_s analysed below.

Further investigations on the daily changes in g_s and Ψ showed that: (1) half-open flowers had generally higher g_s than fully-open flowers, and tepals of half-open flowers in the 3rd whorl had higher g_s than those of the 1st and 2nd whorls (Fig. S3a, b). (2) Leaf g_s initially increased over the morning, peaked around 10:30, and then decreased to near zero for the remainder of the day. Younger leaves (1st leaf) showed higher g_s than mature leaves (Fig. S3c, d). (3) Ψ_{tepal} of half-open flowers was remarkably variable and lacked clear patterns compared to those of fully-open flowers.

459 Ψ_{tepal} of the 1st whorl was more negative than those of the 2nd and 3rd whorls. There
460 were no differences of Ψ_{tepal} between morning and afternoon, or between the two
461 studied species (Fig. S4a, b). (4) Ψ_{leaf} was nearly -0.1 MPa at 7:00, reached its most
462 negative at 13:00, and then returned to around -0.2 MPa at 18:00. There were no
463 differences of Ψ_{leaf} among the four growth stages (Fig. S4c, d). Overall, average Ψ_{leaf}
464 values were more negative than Ψ_{tepal} in both species, and all the Ψ values were above
465 Ψ_{tlp}. Although minimum Ψ in *M. soulangeana* approached average Ψ_{tlp}, specific
466 HSMs remained above zero (Fig. S4, Table 1).
467
468 **Discussion**
469 *Sap flow and stomatal conductance patterns differ between flowers and leaves*
470 Sap flow in the *Magnolia* flowers that we measured showed distinct daily dynamic
471 patterns compared with leaves, with J_S starting early at predawn (or even from 4:00
472 for *M. soulangeana*), quickly peaking midmorning, then decreased the remainder of
473 the day, despite a continuous increase in *D* until 13:00. In contrast, leaf J_S remained
474 linked to *D* throughout the day (Fig. 2). Flowers of most Magnoliaceae species open
475 at night (Dieringer, 1999), probably because their main pollinators are beetles, which
476 are active during the night, while only their secondary pollinators (*i.e.*, bees) are
477 active during the day (Thien 1974). Although high J_S of flowers in the morning was
478 assumed to be associated with low Ψ_{tepal} (Ortuno *et al.* 2006), we show that this is not
479 the case for *Magnolia* species, as Ψ_{tepal} remained high throughout the day (-0.05 ~ -0.2
480 MPa) and did not show dramatically daily changes as in Ψ_{leaf} (-0.1 ~ -0.8 MPa) (Fig.
481 S4). This is perhaps due to lower stomatal or cuticular conductances in tepals
482 compared to leaves, or much higher C_{ft} in tepals than leaves, which could maintain
483 water above turgor (Chapotin *et al.* 2003). At the branch level, we also found that
484 flowers store more water than leaves on the same branches, so that branches do not
485 require high J_S to maintain water balance during flowering period. The buffering
486 effects of water stored in stems, which provided ~10% daily water consumption
487 independent of tree size (Meinzer *et al.* 2004), may similarly explain the low ratio of
488 J_S in flowers to that predicted for leaves (22% and 55% for *M. denudata* and *M.*
489 *soulangeana*, respectively). Therefore, we speculate that the driving forces behind
490 floral J_S might come not only from tepal *E* or Ψ_{tepal} changes during the day, but also
491 from flower opening forces at night and predawn. These forces may include the apical
492 growth (osmotic potential brought by carbohydrates decomposition) during floral

development (Xu and Rudall 2006), floral cuticular conductance brought by thermogenesis (Dieringer 1999; Wang *et al.* 2014), and water needed for the physical expansion of tepals (Wada *et al.* 2004; Azad *et al.* 2007). As we did not measure these physiological activities directly here, we recommend that they be investigated in future studies on floral hydraulics.

The *Magnolia* flowers in our study were more vulnerable to environmental fluctuations than leaves, with floral J_S and g_s presenting different responses to changes in *D* and light (Fig. 4-5). Under low light, flower J_S remained very low and did not respond to increases in *D*, which might result from the buffering effects of stored water within the tepals, as reported for mango inflorescences (Higuchi and Sakuratani 2005). In contrast, the high light of the afternoon caused the J_S of flowers to decrease quickly as *D* increased (Fig. 4), because the higher tepal C_{ft} indicates greater water loss under the same *D* and light stress, i.e., flowers are much more vulnerable to desiccation than leaves. We also noticed that some fully-open flowers started to wilt in the afternoon due to high light or temperature, which caused high *D* and allowed J_S to decrease, leaving water for the half-open flowers and buds the following day. Together, this helps to define the overall flowering phenology at the tree level. Furthermore, in our study species, low LDMC and the high Ψ_{tlp} and C_{ft} of the tepals indicates large vacuoles in their parenchyma cells and high vulnerability to desiccation, similar to orchids flowers (Zhang *et al.* 2017). Then the tepals produce few stomata to help maintain low g_s and Ψ_{tepal} to sustain high HSM and avoid desiccation under normal water conditions. Therefore, due to higher water storage and lower water loss, we found that the absolute value of tepal g_s was only 27~65% that of leaves, and had a shallower slope with ln*D* than leaves (Fig. 5). We also found that the inner whorl of half-open flowers is the primary driver of flower water consumption (*i.e.*, higher Ψ_{tepal} and g_s than the other two whorls, Fig. S3-4; Table S1). While these Ψ_{tepal} findings are consistent with those of *Magnolia grandiflora*, our g_s findings differ such that the 1st whorl of *M. grandiflora* had higher g_s than the 3rd whorl (Feild *et al.* 2009b). One possible reason for this discrepancy may be due to the fully-open flowers that they used, as the g_s in our study showed no differences between the 1st and 3rd whorls for fully-open flowers (Fig. S3), indicating that water consumption strongly depends on flowering stage.

In leaves, *D* and water transpired through gas exchange were clearly the main drivers of water transportation and sap flow, as confirmed by the congruent pattern of

daily leaf J_S, g_s and D (Fig. 1, 2, 4, 5). Many studies address hydraulic regulation as a method to prevent xylem embolism under water stress brought on by atmospheric dryness (high evaporative demand) and/or soil drought (Tyree and Sperry 1989; Nardini *et al.* 2012). Because our study had sufficient soil and stem water supplies, modest increases in D would initially enhance evaporation, E and K_{leaf}. However, Ψ_{leaf} may slightly drop and a continuous decrease in Ψ_{leaf} would cause stomata closure, leading to lower g_s, E and K_{leaf}, such that xylem tensions in the stems could remain within a safe range (Meinzer and Grantz 1990; Brodribb and Holbrook 2004; Franks 2004). Studies at the stand scale show that canopy stomata respond to D via the regulation of g_s and Ψ_{leaf} (Granier and Loustau 1994; Oren *et al.* 1999; Oren *et al.* 2001), which is important to understand water balance within the whole ecosystem. Therefore, co-regulation of Ψ_{leaf}, K_{leaf}, and J_S is the result of the hydraulic-photosynthetic coordination of leaves.

Ecophysiology underpinning the different water relations between flowers and leaves

Flowers of the two *Magnolia* species consumed less water per area (lower E and J_S) than the leaves, while tepals showed lower K_{tepal} but higher K_L than leaves, due to their specific structures. As assimilation organs, we found that leaves had higher LDMC, indicating greater investments in veins and photosynthetic structures than tepals, as is the case for most angiosperm species (Roddy *et al.* 2013). This allocation leads to lower internal resistance and higher intrinsic K_{leaf}, and enables higher rates of transpiration and photosynthesis in leaves (Brodribb *et al.* 2007). Our results were consistent with this hypothesis in LDMC, K_{leaf} or K_{tepal}, and gas exchange traits. Although thick and well-hydrated tepals led to less negative Ψ_{tepal}, their much lower E was more decisive in K_{tepal} compared with K_{leaf}, showing similar K_{leaf} or K_{tepal} values, as was also reported in *Magnolia grandiflora* (Feild *et al.* 2009b). Large, thick, and hydrated tepals are commonly found in Magnoliaceae species that evolved in relatively moist environments (Feild *et al.* 2009a). These tepal phenotypes may effectively protect stamens and gynoecia, attract pollinators (mainly beetles) by colour, fragrance, and thermogenesis under low air temperature (Azuma *et al.* 1999; Dieringer 1999; Wang *et al.* 2014), or even provide food for pollinators (Thien 1974; Gottsberger *et al.* 2012). Moreover, we found that K_S was similar in the flowers and leaves of our study species, but that flower K_L was higher than that of leaves due to the considerably lower A_L/A_S of flowers (Table 1). These findings confirm that stems

561 are hydraulically built to accommodate the high transpiration by leaves and, as such,
562 are hydraulically overbuilt for flowers. Stem xylem conduits are the structural basis of
563 K_S (Sperry *et al.* 2008), and these should not change appreciably during our two-
564 month experimental period. As the maximum hydraulic conductivity, K_S is suitable to
565 compare hydraulic conductivity potential rather than water transport situation *in situ*.
566 Therefore, while K_S and K_L values only showed different maximum hydraulic
567 conductivity between tepals and leaves, the *in situ* hydraulic differences could be
568 represented by K_{leaf} or K_{tepal}, g_s, E, Ψ, and J_S at leaf or tepal and branch levels, with
569 Ψ_{tlp} as a reference to assess HSM, which was always positive under our study
570 conditions.

571 In the two *Magnolia* species studied here, stomata were larger and lower density on
572 the tepals than the leaves, which constrains stomatal conductance, leading to very low
573 absolute values of g_s and E in the flowers. This prevents water loss and helps to
574 maintain the water balance of flowers through stomatal adjustments (Franks and
575 Beerling 2009). Thus under naturally varying environmental conditions, all tepals of
576 fully-open and half-open flowers experienced water potentials higher than Ψ_{tlp} (i.e.,
577 positive HSM in Fig. S4). Meanwhile, floral J_S was much less than leaves based on
578 both experimental data (Fig. 2) and simulated values (Fig. S1). Previous studies found
579 that floral stomata of several orchid species were dysfunctional and did not transpire
580 (Hew *et al.* 1980). However, our study found higher opening ratios in tepals than
581 leaves and that tepal g_s was about 27~65% that of leaves, firmly indicating the
582 functionality of tepal stomata. The relatively high g_s might also be affected by
583 evaporation through the epidermis and cuticle in the leaf chamber during gas
584 exchange measurements, which is likely much higher in flowers (30-90 mmol m^{-2} s^{-1}
585 for magnoliids) than in leaves (Roddy *et al.* 2016). Consistent with our findings (Fig.
586 S3), E of avocado flowers is 60-80% of nearby leaves, peaking in the early morning
587 and dramatically declining midday (Whiley *et al.* 1988; Blanke and Lovatt 1993).

588 Considering the brief flowering period (7~10 days) and remarkably short lifespan
589 of each tepal (2~3 days) in *Magnolia* species, it should be more economical for the
590 whole plant to invest less water and carbon in the non-photosynthetic tepals (per unit
591 area). This was supported by our study, which found that flowers had lower J_S, E, and
592 LDMC in flowers than leaves. The strong selection pressures for greater hydraulic
593 conductance in leaves within developed angiosperm families did not exist for flowers
594 (Brodribb and Feild 2010; Roddy *et al.* 2013), especially in basal angiosperms like the

Magnoliaceae that evolved in wet habitats lacking hydraulic limitations (Feild *et al.* 2009a). This is consistent with a recent study that found basal angiosperm flowers maintain higher K_{flower} due to traits related with high rates of water loss and supply (Roddy *et al.* 2016).

Conclusion

This study demonstrated different water relations for flowers and leaves of two flower-before-leaf-emergence *Magnolia* species. The ratio of J_S in flowers to that predicted for leaves during the flowering period was 22% and 55% for *M. denudata* and *M. soulangeana*, respectively. J_S in flowers began before predawn and ceased early in the afternoon due to night-flowering and high sensitivity of g_s to D, indicating that stomata closed early to save water before cavitation occurred. Thus, we propose that the strongest driving forces of flower J_S might include Ψ_{tepal} and/or transpiration, as well as other physiological processes during flowering, such as apical growth, thermogenesis, and tepal expansion. In addition, flower water loss happened mainly in the center of the flower and greatly depended on flowering stages. We then explored the ecophysiological basis of the differences in water relations between leaves and flowers, finding that tepals were thicker, more hydrated, had lower LDMC, and had larger and less dense stomata, which lead to lower g_s, g_{max}, E, and K_{tepal}, less negative Ψ_{tepal} and Ψ_{tlp}, and higher K_L than these traits in leaves. This study showed that to keep constant Ψ and avoid losing water before cavitation, tepals maintain lower hydraulic conductance than leaves, while leaves had more efficient stomatal responses to D than tepals. Consequently, flowers consumed less than half the water that leaves did at both the tepal, leaf, and branch levels for both species. Our study examined water consumption and the ecophysiological basis between flowers and leaves in two *Magnolia* species, which we hope will inspire future investigations on floral hydraulics.

Appendix

An appendix is available online and consists of the following:

Table S1: Morphological and ecophysiological traits with significant differences among three tepal whorls or four leaf growth stages of *M. denudata* and *M. soulangeana*.

Fig. S1: Predicted J_S of leaves during the flowering period based on the relationships between J_S and D, using D from Feb-24 for *M. denudata* and *M. soulangeana*.

Fig. S2: Flower or leaf areas versus stem diameters for *M. denudata* and *M. soulangeana*.

Fig. S3. Daily changes in flower and leaf stomatal conductance (g_s) of *M. denudata* and *M. soulangeana* during two sunny days with either only flowers or leaves on the tree, respectively.

Fig. S4. Daily changes in flower and leaf water potential (Ψ) of *M. denudata* and *M. soulangeana* during two sunny days with either only flowers or leaves on the tree, respectively.

Acknowledgements

We are grateful to Prof. Ram Oren from Duke University for constructive comments on the manuscript. We appreciate Keming Yang in the Horticulture Center in South China Botanical Garden for his help in selecting species and available trees. We also thank Ronghua Li, Pengcheng He, Guoliang Ye, Lei Hua, Shidan Zhu and Hui Zhang for their technical assistant. This work was funded by the National Natural Science Foundation of China (31670411), and the National Basic Research Program of China (2013CB956704). The authors declare no conflicts of interest.

References

Azad, AK, Sawa, Y, Ishikawa, T, Shibata, H (2007) Temperature-dependent stomatal movement in tulip petals controls water transpiration during flower opening and closing. *Annals of Applied Biology* **150**, 81-87.

Azuma, H, García-Franco, JG, Rico-Gray, V, Thien, LB (2001) Molecular phylogeny of the Magnoliaceae: the biogeography of tropical and temperate disjunctions. *American Journal of Botany* **88**, 2275-2285.

Azuma, H, Thien, LB, Kawano, S (1999) Floral scents, leaf volatiles and thermogenic flowers in Magnoliaceae. *Plant Species Biology* **14**, 121-127.

Blanke, MM, Lovatt, CJ (1993) Anatomy and transpiration of the avocado inflorescence. *Annals of Botany* **71**, 543-547.

659 Brodribb, T, Holbrook, NM (2004) Diurnal depression of leaf hydraulic conductance in a
660 tropical tree species. *Plant, Cell & Environment* **27**, 820-827.
661 Brodribb, TJ, Feild, TS (2010) Leaf hydraulic evolution led a surge in leaf photosynthetic
662 capacity during early angiosperm diversification. *Ecology Letters* **13**, 175-183.
663 Brodribb, TJ, Feild, TS, Jordan, GJ (2007) Leaf maximum photosynthetic rate and venation
664 are linked by hydraulics. *Plant Physiology* **144**, 1890-1898.
665 Brodribb, TJ, Holbrook, NM (2003) Changes in leaf hydraulic conductance during leaf
666 shedding in seasonally dry tropical forest. *New Phytologist* **158**, 295–303.
667 Brown, HT, Escombe, F (1900) Static diffusion of gases and liquids in relation to the
668 assimilation of carbon and translocation in plants. *Proceedings of the Royal Society of*
669 *London* **67**, 124-128.
670 Chambers, JL, Hinckley, TM, Cox, GS, Metcalf, C, Aslin, R (1985) Boundary-line analysis
671 and models of leaf conductance for 4 oak-hickory forest species. *Forest Science* **31**, 437-
672 450.
673 Chapotin, S, Holbrook, N, Morse, S, Gutierrez, M (2003) Water relations of tropical dry
674 forest flowers: pathways for water entry and the role of extracellular polysaccharides.
675 *Plant, Cell & Environment* **26**, 623-630.
676 Dandy, JE (1927) The genera of Magnoliaceae. *Kew Bulletin* **7**, 257-264.
677 Dieringer, G (1999) Beetle pollination and floral thermogenicity in *Magnolia tamaulipana*
678 (Magnoliaceae). *International Journal of Plant Sciences* **160**, 64-71.
679 Ewers, B, Gower, S, Bond-Lamberty, B, Wang, C (2005) Effects of stand age and tree species
680 on canopy transpiration and average stomatal conductance of boreal forests. *Plant, Cell &*
681 *Environment* **28**, 660-678.
682 Feild, TS, Chatelet, DS, Brodribb, TJ (2009a) Ancestral xerophobia: a hypothesis on the
683 whole plant ecophysiology of early angiosperms. *Geobiology* **7**, 237-264.
684 Feild, TS, Chatelet, DS, Brodribb, TJ (2009b) Giant flowers of Southern magnolia are
685 hydrated by the xylem. *Plant Physiology* **150**, 1587-1597.
686 Figlar, RB, Nooteboom, HP (2004) Notes on Magnoliaceae IV. *Blumea* **49**, 87-100.

687 Franks, PJ (2004) Stomatal control and hydraulic conductance, with special reference to tall
688 trees. *Tree Physiology* **24**, 865-878.
689 Franks, PJ, Beerling, DJ (2009) Maximum leaf conductance driven by CO_2 effects on
690 stomatal size and density over geologic time. *Proceedings of the National Academy of*
691 *Sciences* **106**, 10343-10347.
692 Galen, C, Sherry, RA, Carroll, AB (1999) Are flowers physiological sinks or faucets? Costs
693 and correlates of water use by flowers of *Polemonium viscosum*. *Oecologia* **118**, 461-470.
694 Gottsberger, G, Silberbauer-Gottsberger, I, Seymour, RS, Dötterl, S (2012) Pollination
695 ecology of *Magnolia ovata* may explain the overall large flower size of the genus. *Flora-*
696 *Morphology, Distribution, Functional Ecology of Plants* **207**, 107-118.
697 Granier, A, Loustau, D (1994) Measuring and modelling the transpiration of a maritime pine
698 canopy from sap-flow data. *Agricultural and Forest Meteorology* **71**, 61-81.
699 Gross, KL, Soule, JD (1981) Differences in biomass allocation to reproductive and vegetative
700 structures of male and female plants of a dioecious, perennial herb, *Silene alba* (Miller)
701 Krause. *American Journal of Botany* 801-807.
702 Hew, CS, Lee, GL, Wong, SC (1980) Occurrence of Non-functional Stomata in the Flowers
703 of Tropical Orchids. *Annals of Botany* **46**, 195-201.
704 Higuchi, H, Sakuratani, T (2005) The sap flow in the peduncle of the mango (*Mangifera*
705 *indica* L.) inflorescence as measured by the stem heat balance method. *Journal of the*
706 *Japanese Society of Horticultural Science* **74**, 109-114.
707 Kim, S, Suh, Y (2013) Phylogeny of Magnoliaceae based on ten chloroplast DNA regions.
708 *Journal of Plant Biology* **56**, 290-305.
709 Lambrecht, S, Dawson, T (2007) Correlated variation of floral and leaf traits along a moisture
710 availability gradient. *Oecologia* **151**, 574-583.
711 Lambrecht, SC (2013) Floral water costs and size variation in the highly selfing *Leptosiphon*
712 *bicolor* (Polemoniaceae). *International Journal of Plant Sciences* **174**, 74-84.
713 Lambrecht, SC, Santiago, LS, DeVan, CM, Cervera, JC, Stripe, CM, Buckingham, LA,
714 Pasquini, SC (2011) Plant water status and hydraulic conductance during flowering in the

715 southern California coastal sage shrub *Salvia mellifera* (Lamiaceae). *American Journal of*
716 *Botany* **98**, 1286-1292.
717 Law, YW (2004) Magnolias of China. Beijing Sciences & Technology Press, Beijing.
718 Liu, H, Lundgren, MR, Freckleton, RP, Xu, QY, Ye, Q (2016) Uncovering the spatio-
719 temporal drivers of species trait variances: a case study of Magnoliaceae in China. *Journal*
720 *of Biogeography* **43**, 1179-1191.
721 Liu, YH, Zhou, RZ, Zeng, QW (1997) *Ex situ* conservation of Magnoliaceae including its
722 area and endangered species. *Journal of Tropical and Subtropical Botany* **5**, 1-12. (in
723 Chinese).
724 Lohammar, T, Larsson, S, Linder, S, Falk, SO (1980) FAST: simulation models of gaseous
725 exchange in Scots pine. *Ecological Bulletins* 505-523.
726 Meinzer, F, Grantz, D (1990) Stomatal and hydraulic conductance in growing sugarcane:
727 stomatal adjustment to water transport capacity. *Plant, Cell & Environment* **13**, 383-388.
728 Meinzer, FC, James, SA, Goldstein, G (2004) Dynamics of transpiration, sap flow and use of
729 stored water in tropical forest canopy trees. *Tree Physiology* **24**, 901-909.
730 Munguía-Rosas, MA, Ollerton, J, Parra-Tabla, V, De-Nova, JA (2012) Meta-analysis of
731 phenotypic selection on flowering phenology suggests that early flowering plants are
732 favoured. *Ecology Letters* **14**, 511-521.
733 Nardini, A, Pedà, G, Rocca, NL (2012) Trade-offs between leaf hydraulic capacity and
734 drought vulnerability: morpho-anatomical bases, carbon costs and ecological
735 consequences. *New Phytologist* **196**, 788-798.
736 Oren, R, Sperry, J, Ewers, B, Pataki, D, Phillips, N, Megonigal, J (2001) Sensitivity of mean
737 canopy stomatal conductance to vapor pressure deficit in a flooded *Taxodium distichum* L.
738 forest: hydraulic and non-hydraulic effects. *Oecologia* **126**, 21-29.
739 Oren, R, Sperry, J, Katul, G, Pataki, D, Ewers, B, Phillips, N, Schäfer, K (1999) Survey and
740 synthesis of intra- and interspecific variation in stomatal sensitivity to vapour pressure
741 deficit. *Plant, Cell & Environment* **22**, 1515-1526.

742 Ortuno, MF, García-Orellana, Y, Conejero, W, Ruiz-Sánchez, MC, Alarcón, JJ, Torrecillas, A
743 (2006) Stem and leaf water potentials, gas exchange, sap flow, and trunk diameter
744 fluctuations for detecting water stress in lemon trees. *Trees* **20**, 1-8.
745 Qiu, YL, Lee, J, Bernasconi-Quadroni, F, Soltis, DE, Soltis, PS, Zanis, M, Zimmer, EA,
746 Chen, Z, Savolainen, V, Chase, MW (1999) The earliest angiosperms: evidence from
747 mitochondrial, plastid and nuclear genomes. *Nature* **402**, 404-407.
748 R Development Core Team (2013) 'R: A language and environment for statistical computing.'
749 (R Foundation for Statistical Computing: Vienna, Austria)
750 Reekie, E, Bazzaz, F (1987) Reproductive effort in plants. 3. Effect of reproduction on
751 vegetative activity. *American Naturalist* 907-919.
752 Roddy, A, Dawson, T (2012) Determining the water dynamics of flowering using miniature
753 sap flow sensors. *Acta Horticulturae* **951**, 47-53.
754 Roddy, AB, Brodersen, CR, Dawson, TE (2016) Hydraulic conductance and the maintenance
755 of water balance in flowers. *Plant, Cell & Environment* **39**, 2123-2132.
756 Roddy, AB, Guilliams, CM, Lilittham, T, Farmer, J, Wormser, V, Pham, T, Fine, PV, Feild,
757 TS, Dawson, TE (2013) Uncorrelated evolution of leaf and petal venation patterns across
758 the angiosperm phylogeny. *Journal of Experimental Botany* **64**, 4081-4088.
759 Sack, L, Cowan, PD, Jaikumar, N, Holbrook, NM (2003) The 'hydrology' of leaves: co-
760 ordination of structure and function in temperate woody species. *Plant Cell &*
761 *Environment* **26**, 1343-1356.
762 Sack, L, Melcher, PJ, Zwieniecki, MA, Holbrook, NM (2002) The hydraulic conductance of
763 the angiosperm leaf lamina: a comparison of three measurement methods. *Journal of*
764 *Experimental Botany* **53**, 2177-2184.
765 Sakuratani, T (1981) A heat balance method for measuring water flux in the stem of intact
766 plants. *Journal of Agricultural Meteorology* **37**, 9-17.
767 Schulte, PJ, Hinckley, TM (1985) A comparison of pressure-volume curve data analysis
768 techniques. *Journal of Experimental Botany* **36**, 1590-1602.

769 Seymour, RS, White, CR, Gibernau, M (2003) Environmental biology: heat reward for insect
770 pollinators. *Nature* **426**, 243-244.
771 Sperry, JS, Meinzer, FC, McCulloh, KA (2008) Safety and efficiency conflicts in hydraulic
772 architecture: scaling from tissues to trees. *Plant, Cell & Environment* **31**, 632-645.
773 Teixido, AL, Valladares, F (2014) Disproportionate carbon and water maintenance costs of
774 large corollas in hot Mediterranean ecosystems. *Perspectives in Plant Ecology Evolution*
775 *& Systematics* **16**, 83-92.
776 Thien, LB (1974) Floral biology of *Magnolia*. *American Journal of Botany* **61**, 1037-1045.
777 Thien, LB, Azuma, H, Kawano, S (2000) New perspectives on the pollination biology of
778 basal angiosperms. *International Journal of Plant Sciences* **161**, S225-S235.
779 Thien, LB, Bernhardt, P, Devall, MS, Chen, Z-d, Luo, Y-b, Fan, J-H, Yuan, L-C, Williams,
780 JH (2009) Pollination biology of basal angiosperms (ANITA grade). *American Journal of*
781 *Botany* **96**, 166-182.
782 Tyree, M, Hammel, H (1972) The measurement of the turgor pressure and the water relations
783 of plants by the pressure-bomb technique. *Journal of Experimental Botany* **23**, 267-282.
784 Tyree, MT, Sperry, JS (1989) Vulnerability of xylem to cavitation and embolism. *Annual*
785 *review of plant biology* **40**, 19-36.
786 Wada, H, Iwaya-Inoue, M, Akita, M, Nonami, H (2004) Direct measurements of cell turgor
787 and hydraulic conductance in expanding tulip (*Tulipa gesneriana* L.) tepals. *Environment*
788 *Control in Biology (Japan)* **42**, 205-215.
789 Wang, R, Xu, S, Liu, X, Zhang, Y, Wang, J, Zhang, Z (2014) Thermogenesis, flowering and
790 the association with variation in floral odour attractants in *Magnolia sprengeri*
791 (Magnoliaceae). *PloS one* **9**, e99356.
792 Whiley, A, Chapman, K, Saranah, J (1988) Water loss by floral structures of avocado (*Persea*
793 *americana* cv. Fuerte) during flowering. *Australian Journal of Agricultural Research* **39**,
794 457-467.
795 Xu, F, Rudall, P (2006) Comparative floral anatomy and ontogeny in Magnoliaceae. *Plant*
796 *Systematics and Evolution* **258**, 1-15.

Zhang, F-P, Brodribb, TJ (2017) Are flowers vulnerable to xylem cavitation during drought? *Proceedings of the Royal Society B: Biological Sciences* **284**,

Zhang, F-P, Yang, Y-J, Yang, Q-Y, Zhang, W, Brodribb, TJ, Hao, G-Y, Hu, H, Zhang, S-B (2017) Floral mass per area and water maintenance traits are correlated with floral longevity in Paphiopedilum (Orchidaceae). *Frontiers in Plant Science* **8**,

Table 1. Morphological and ecophysiological traits of flowers and leaves of *Magnolia denudata* and *Magnolia soulangeana*, with results of *t*-tests for each trait. Data are mean ± SEM, and natural log-transformed in models. Sample sizes (n) of flower or leaf traits are the same for *M. denudata* and *M. soulangeana*, therefore only sample sizes for *M. denudata* are given in brackets. Differences between flowers and leaves for each trait were analysed using *t*-tests (* $P<0.05$; ** $P<0.01$; *** $P<0.001$; ns, not significant), "-" indicates *t*-tests are not applicable, "†" indicates significant differences among three whorls of flowers, or four leaf growth stages by ANOVA, which are reported and further analyzed in the Appendix. Abbreviations: DBH, diameter at breast height; WD, sapwood density; A_L/A_S, leaf to sapwood area ratio; SLA, specific leaf (or tepal) area; LDMC, leaf (or tepal) dry matter content; SPI, stomatal pore area index; g_{max}, maximum stomatal conductance to water vapour; g_s, stomatal conductance; E, transpiration rate; Ψ_{am}, leaf (or tepal) water potential at 10:30~11:00; Ψ_{pm}, leaf (or tepal) water potential at 16:00~16:30; Ψ_{tlp}, turgor loss point; HSM, hydraulic safety margin; C_{ft}, capacitance at full turgor; K_{leaf} or K_{tepal}, leaf (or tepal) hydraulic conductance; K_S, sapwood specific hydraulic conductivity; K_L, leaf (or tepal) specific hydraulic conductivity.

	Magnolia denudata			*Magnolia soulangeana*		
	Flower (*n*)	Leaf (*n*)	*t*-test	Flower	Leaf	*t*-test
Tree height (m)	8.48 ± 0.51 (5)		-	7.42 ± 0.68		-
DBH (cm)	16.63 ± 0.44 (5)		-	12.91 ± 0.62		-
WD (g cm^{-3})	0.42 ± 0.02 (5)		-	0.47 ± 0.01		-
Single tepal or leaf area (cm^2)	20.62 ± 1.07 (18)	58.35 ± 3.61 (24) †	***	42.57 ± 3.61 †	58.69 ± 4.12 †	***
A_L/A_S (m^2 cm^{-2})	0.17 ± 0.04 (5)	0.62 ± 0.05 (5)	***	0.22 ± 0.03	0.71 ± 0.06	***
Tepal or leaf thickness (mm)	2.12 ± 0.17 (18) †	0.15 ± 0.00 (24) †	***	2.17 ± 0.27 †	0.14 ± 0.00 †	***
Tepal thinnest thickness (mm)	0.20 ± 0.01 (18)		-	0.21 ± 0.02 †		-

SLA ($cm^2\ g^{-1}$)	258.23 ± 24.12 (18)	335.31 ± 6.43 (12)	***	323.34 ± 24.22	352.43 ± 12.01	*
LDMC (%)	6.09 ± 0.15 (18) †	17.32 ± 0.31 (12)	***	6.24 ± 0.11 †	18.28 ± 0.45	***
N (%)	2.97 ± 0.02 (9)	2.86 ± 0.08 (12)	ns	2.62 ± 0.13	2.62 ± 0.06	ns
P (%)	0.38 ± 0.02 (9)	0.35 ± 0.01 (12)	ns	0.36 ± 0.01	0.34 ± 0.02	ns
Abaxial stomatal size (μm^2)	875.62 ± 47.05 (18)	561.22 ± 12.89 (24)	***	864.48 ± 36.46	513.65 ± 13.55	***
Adaxial stomatal size (μm^2)	998.68 ± 57.32 (18)		-	918.11 ± 44.60		-
Stomatal density (number mm^{-2})	3.08 ± 0.31 (36)	277.33 ± 8.09 (24)	***	2.11 ± 0.22	244.67 ± 7.05	***
SPI (%)	1.00 ± 0.06 (18)	30.49 ± 1.00 (24)	***	0.65 ± 0.04	22.80 ± 0.63	***
g_{max} ($mol\ m^{-2}\ s^{-1}$)	0.07 ± 0.00 (18)	2.93 ± 0.09 (24)	***	0.05 ± 0.00	2.31 ± 0.06	***
g_s ($mol\ m^{-2}\ s^{-1}$)	0.021±.002 (120) †	0.078±.008 (120) †	***	0.041 ± .003 †	0.063 ± .003 †	***
E ($mmol\ m^{-2}\ s^{-1}$)	0.28 ± 0.02 (120) †	1.30 ± 0.10 (120) †	***	0.51 ± 0.03 †	0.93 ± 0.05 †	***
Ψ_{am} (MPa)	-0.15 ± 0.02 (18) †	-0.35 ± 0.05 (12)	***	-0.13 ± 0.03 †	-0.53 ± 0.05	***
Ψ_{pm} (MPa)	-0.11 ± 0.02 (18) †	-0.57 ± 0.05 (12)	***	-0.08 ± 0.01 †	-0.76 ± 0.02	***
Ψ_{tlp} (MPa)	-0.27 ± 0.02 (18)	-0.82 ± 0.02 (12)	***	-0.22 ± 0.03 †	-0.77 ± 0.03	***
HSM (MPa)	0.12 ± 0.01 (18) †	0.24 ± 0.02 (12)	***	0.11 ± 0.03 †	0.02 ± 0.01	***
C_{ft} ($mol\ m^{-2}\ MPa^{-1}$)	6.01 ± 0.48 (18)	0.78 ± 0.03 (12)	***	6.77 ± 1.45 †	0.60 ± 0.04	***
K_{leaf} or K_{tepal} ($mmol\ m^{-2}\ s^{-1}\ MPa^{-1}$)	4.13 ± 0.70 (18) †	14.46 ± 1.23 (12) †	***	4.81 ± 0.83 †	12.11 ± 1.54 †	***
K_S ($kg\ m^{-1}\ s^{-1}\ MPa^{-1}$)	4.37 ± 0.34 (10)	3.73 ± 0.44 (10)	ns	2.16 ± 0.42	2.33 ± 0.35	ns
K_L ($10^{-4}\ kg\ m^{-1}\ s^{-1}\ MPa^{-1}$)	30.60 ± 6.24 (10)	4.42 ± 0.58 (10)	***	8.75 ± 1.24	3.76 ± 0.82	***

Figure Legends

Fig. 1. Daily changes of (a) vapour pressure deficit (*D*, closed circles) and solar radiation (SR, open circles), (b) temperature (black triangles) and rainfall (black bars), sap flux density (J_S) of (c) *Magnolia denudata* and (d) *Magnolia soulangeana*, indicating the flowering and vegetative periods as grey areas in Feb and Mar, respectively. The day that we carried out daily change measurements are marked as D1 and D2 in panels (c) and (d).

Fig. 2. Daily curves of (a) vapour pressure deficit (*D*), (b) solar radiation (SR), and sap flux density (J_S) of (c) *M. denudata* and (d) *M. soulangeana* on two sunny days with only flowers (Feb-24, white dots) or only leaves (Mar-26, black dots) on the tree.

Fig. 3. Flower opening (a, b) and fading (c, d) stages for *M. denudata* and *M. soulangeana*, respectively. Flower number records are based on the 16 branches used for sap flow monitoring (n = 6 for *M. denudata*; n = 10 for *M. soulangeana*), data are mean ± SEM. Grey areas in (a) and (b) indicate flowering periods with stable ratios for both opening and fading stages.

Fig. 4. Sap flux density (J_S) in relation to daytime vapour pressure deficit (*D*) during the flowering (a, b) and vegetative (c, d) periods for *M. denudata* and *M. soulangeana*, respectively. Grey crosses show raw data in ten minutes intervals from days when flower opening ratios were stable and all leaves were expanded, as indicated by grey areas in Figs 1 and 3, with data from rainy days, under limiting light (SR=0 W m^{-2}) and during low *D* (<0.1 kPa) filtered out. Boundary line analyses give the maximum J_S at different SR gradients as low light (LL, black triangles/circles, solid lines, SR=0~400 W m^{-2}) and high light (HL, white triangles/circles, dash lines, SR=400~800 W m^{-2}). The relationships between J_S and ln*D* are: (a) *M. denudata* flower, LL, not modelled; HL, J_S=15.17-24.70×ln*D*; (b) *M. soulangeana* flower, LL, not modelled; HL, J_S=47.31-80.38×ln*D*; (c) *M. denudata* leaf, LL, J_S=50.41+28.25×ln*D*; HL, J_S=96.87+42.10×ln*D*; and (d) *M. soulangeana* leaf, LL, J_S=39.94+18.43×ln*D*; HL, J_S=73.39+4.45×ln*D*.

Fig. 5. Stomatal conductance (g_s) of flower (a, b) and leaf (c, d) in relation to air vapour pressure deficit (*D*) in the morning and afternoon of two sunny days,

847 respectively. The relationships between g_s and ln$D$ are modelled for *M. denudata*
848 (white triangles/circles, dashed lines) and *M. soulangeana* (black triangles/circles,
849 solid lines) separately: (a) *M. denudata*, g_s=0.05-0.09×ln$D$; *M. soulangeana*, g_s=0.08-
850 0.18×ln$D$; (b) *M. denudata*, g_s=0.05-0.11×ln$D$; *M. soulangeana*, g_s=0.09-0.21×ln$D$;
851 (c) *M. denudata*, g_s=0.26-0.54×ln$D$; *M. soulangeana*, g_s=0.10-0.19×ln$D$; and (d) *M.*
852 *denudata*, g_s=0.34-0.33×ln$D$; *M. soulangeana*, g_s=0.12-0.10×ln$D$. Note the axes
853 scales differ in each figure.
854
855

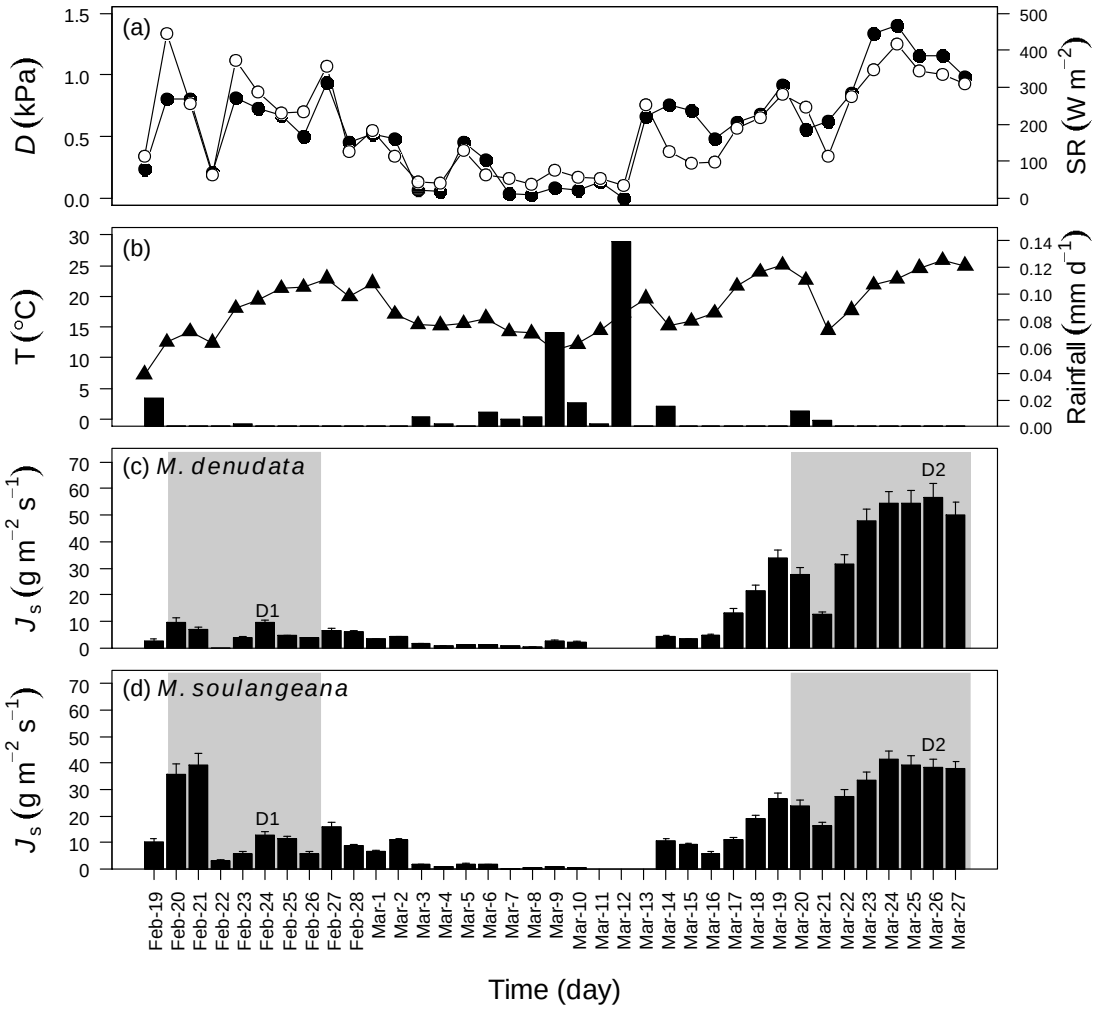

856

857 **Fig. 1. Liu *et al.***

858

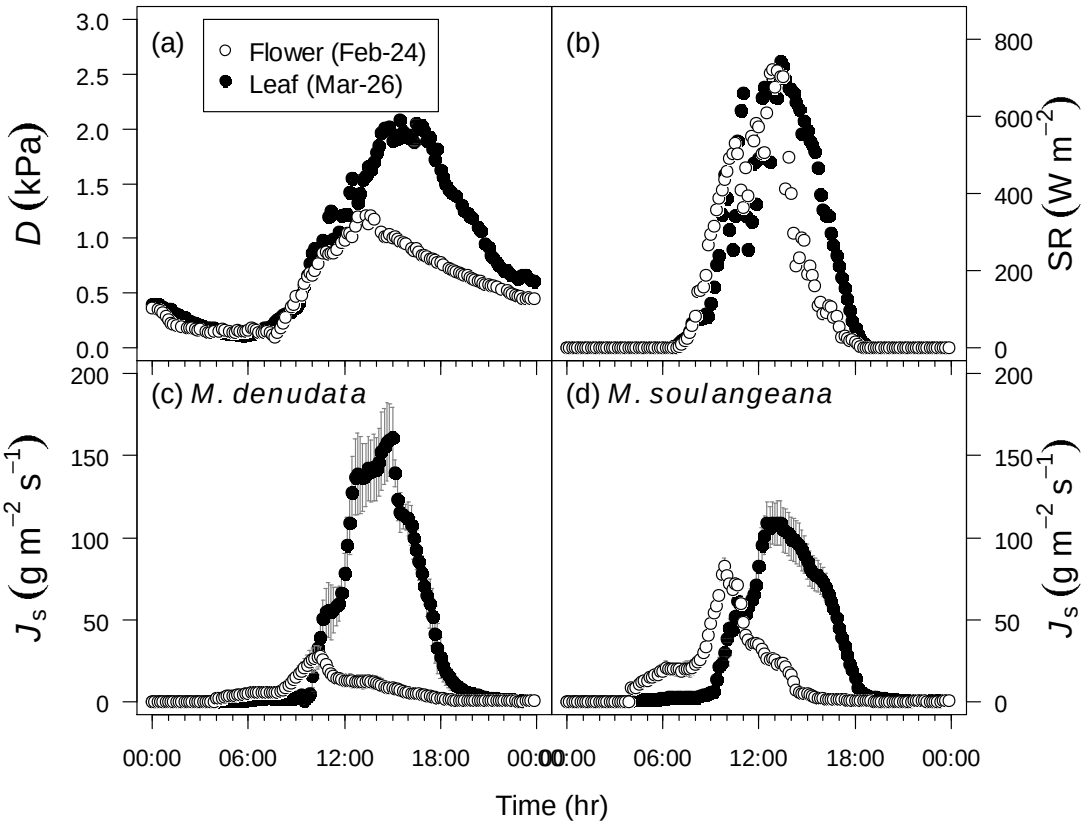

859

860 **Fig. 2. Liu *et al.***

861

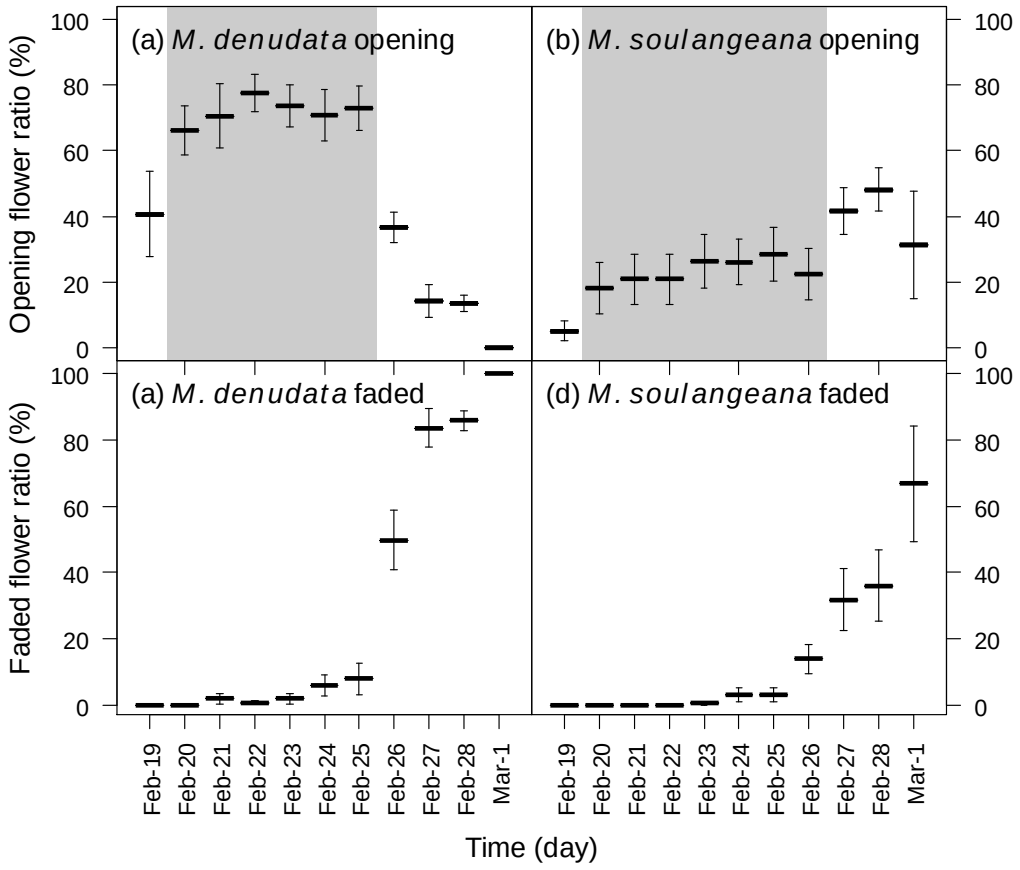

862

863 **Fig. 3. Liu *et al.***

864

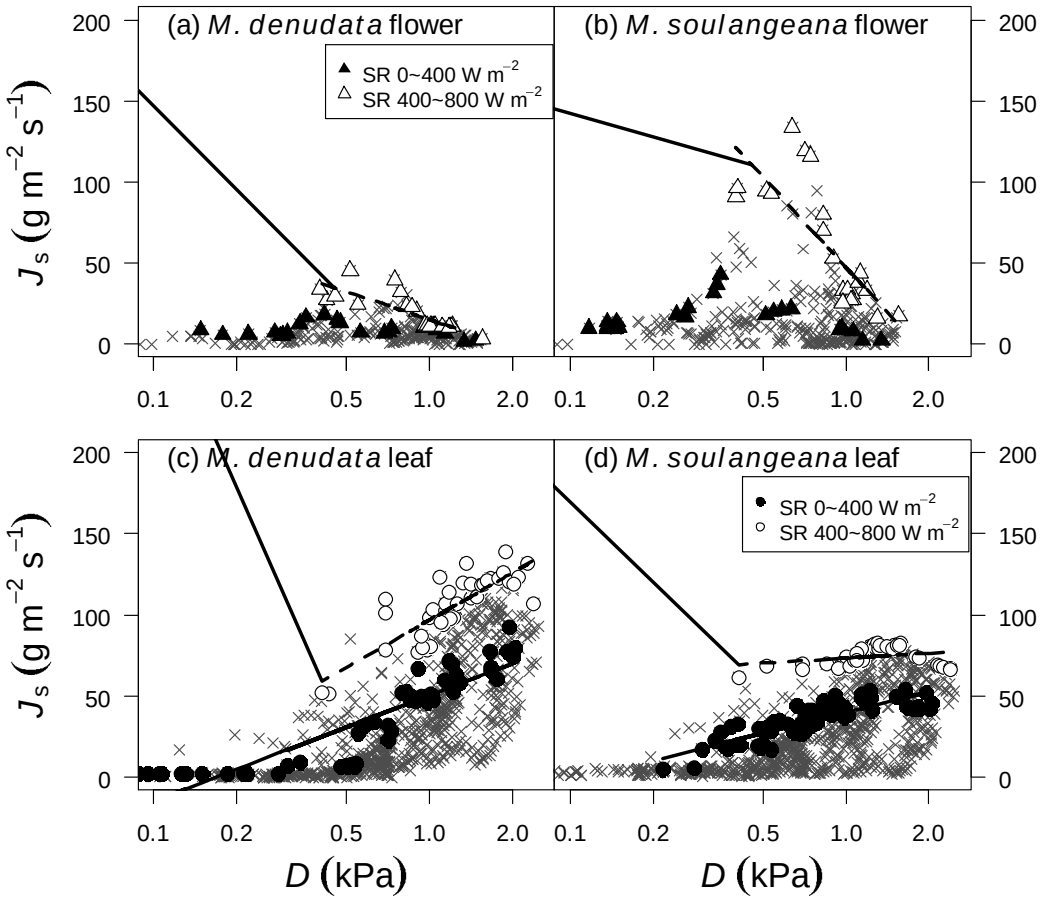

865
866 **Fig. 4. Liu *et al.***

867

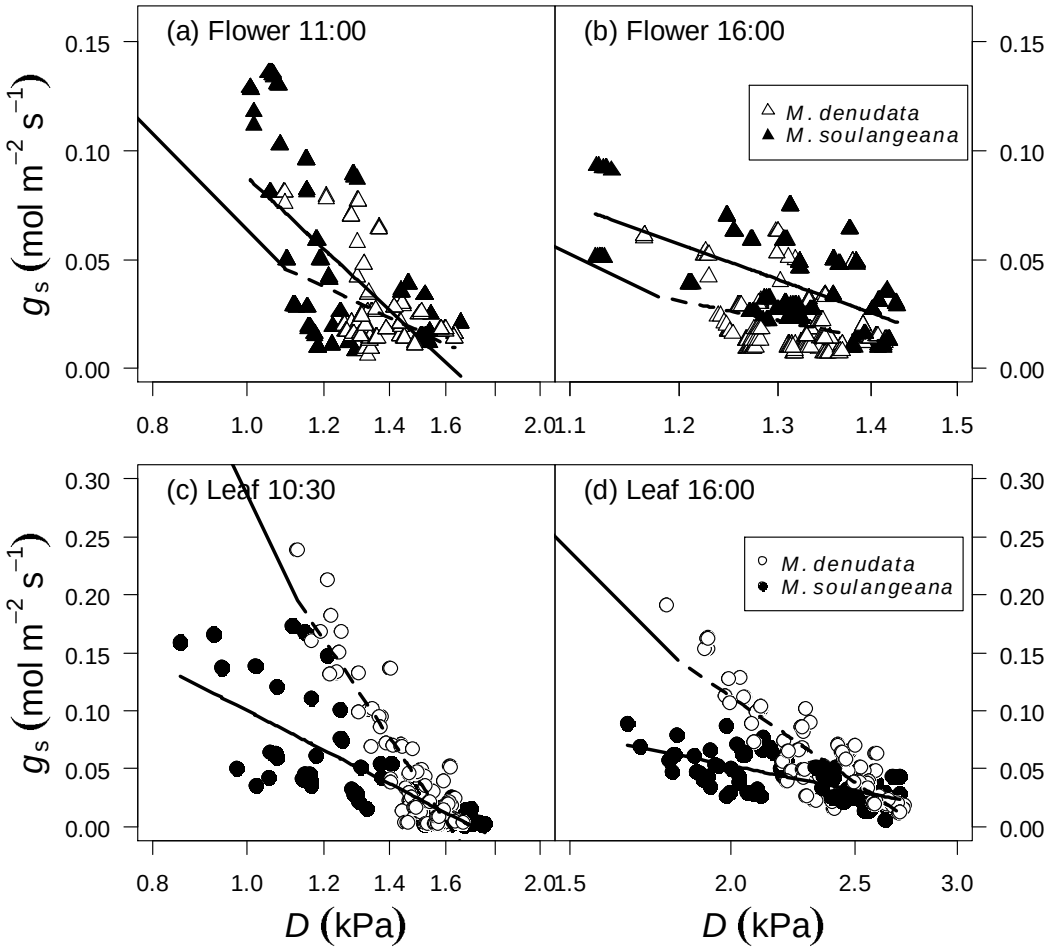

868

869 **Fig. 5. Liu *et al.***

870